Charge distribution in a simulated alkali silicate glass from charge-transfer molecular dynamics

Luis Guillermo Cota*
Facultad de Química, UNAM, Ciudad Universitaria, 04510, México, D. F.

Luis Javier Alvarez†
Instituto de Matemáticas, Unidad Cuernavaca, UNAM, Av. Universidad s/n, Lomas de Chamilpa, Cuernavaca 62210, Morelos, México

Charge-transfer molecular dynamics simulations of quench-free amorphous Li_2O-$4SiO_2$ were carried out in the microcanonical ensemble, at 300K. Distinct oxygen functionalities, such as tricoordinated, dangling and free oxygens, evolved naturally from bridging oxygens in our simulations, upon the addition of the alkali oxide. Discrimination between different structural functionalities becomes straightforward by using charge criterions.

Introduction

In a simulated SiO_2 glass, all oxygens form a "bridge" between two silicon atoms. However, upon the addition of a foreign alkali oxide, such as Li_2O, Si-O-Si bridges break up, generating in the process a number of non-bridging oxigens (herein called "dangling" oxygens) roughly equal to the amount of alkali cations introduced. This fact is substantiated by experimental and theoretical evidence[1,2,3,4]. Whereas most MD authors take the existence of dangling oxygens into account based on proximity or geometric criteria[2,5,6], others incorporate them *a priori* in their simulations[4]. In the search for a more general approach, however, it is desirable to count with a methodology which permits a natural treatment of the different moieties of oxygen in MD simulations.

Computational details

The charge transfer (CT) MD scheme devised by Alavi *et al.*[7] provides the appropriate framework in which, as charge of every atom is a function of its local environment, it is possible to establish a correspondence between charge and structural role. According to the CT model, the total Coulombian energy of a system comprised of N atoms, or particles, is given by

$$V_C(\mathbf{r_1},\mathbf{r_2},\Lambda\ ,\mathbf{r_n}) = \sum_{i=1}^{N-1}\sum_{j=i+1}^{N}\frac{q_i(\mathbf{r_1},\mathbf{r_2},\Lambda\ ,\mathbf{r_n})q_j(\mathbf{r_1},\mathbf{r_2},\Lambda\ ,\mathbf{r_n})}{r_{ij}},$$

* lgc@labvis.unam.mx.

† lja@matcuer.unam.mx.

where

$$q_i = q_i^0 + \frac{\Delta q}{2} \sum_k \left(1 - \tanh\left(\frac{r_{ik} - r_a}{\xi} \right) \right)$$

Here, q_i and q_i^0 are the actual and initial charges of atom *i,* respectively, and $\mathbf{r_1}$, $\mathbf{r_2}$, **...**, $\mathbf{r_n}$ are the atomics positions; r_{ij} is the interatomic distance beween *i* and *j*. Δq, r_a and ξ are adjustable parameters. In our simulations charge transfer is allowed only between Si and O, whereas lithium charges are held constant. The reader is referred to Ref. 7 for details.

Sample preparation

In an attempt to explore an alternative to the usual melt-quench procedure, the feasibility of a simulated structure prepared entirely at room temperature was tested, as detailed below. The structural comparison between room-temperature samples and melt-quench ones will be the subject of a future report. Preliminary work seems to indicate that the differences are mainly in the medium-range ordering[6].

We departed from a pure amorphous SiO_2 configuration consisting of 648 particles (216 Si and 432 O) to which successive amounts of Li_2O were added. Every stabilised sample was used as the basis for a more concentrated one, until the tetrasilicate concentration was reached. The location of sites in the structure suitable to lodge new Li_2O units was done using a previously developed methodology[8]. The density of the pure silica glass was 2.2 g/cm^3, which corresponds to a cubic computational cell of 21.4003 Å per side. The cell dimensions for lithium silicates were calculated using experimental data[9]. The density of the tetrasilicate glass was 2.29 g/cm^3 and the corresponding cell side was 21.9540 Å. The final system consisted of 810 particles (216 Si, 486 O and 108 Li). Initial charge for Si was +3.2*e*[7], and oxygen charge was adjusted accordingly for charge neutrality. For the tetrasilicate, it amounted to –1.6444*e*. During the simulations, however, these charges evolved to an average of about +1.4*e* for Si and –0.7*e* for O.

Each of the concentration steps was carried out in two phases: a constant-temperature run of 10,000 time steps (10 ps) followed by a constant-energy run of typically 15,000 steps. The final preparation (tetrasilicate) was additionally subjected to 50,000 time steps of constant-energy relaxation. It must be pointed out, as regards the thermodynamic equilibrium of the sample, that, it being a glass, its equilibrium is necessarily metastable. However, its structural features persist within the timescale of our simulations. Data collection for statistical analysis was carried out every 1,000 time-step intervals during 50,000 time steps. Radial distribution peak distances were located at 3.17 Å for Si-Si, 1.60 Å for Si-O, 3.20 Å for Si-Li, 2.50 Å for O-O, 2.25 Å for Li-O and 3.20 Å for Li-Li for the tetrasilicate sample (graphs not shown).

Results and discussion

Charge distribution

In a typical simulated SiO_2 glass all oxygens have the same structural (bridging) function. Therefore, it is to be expected that their charges are much alike. This is made evident in Fig.1, where the charge histogram of the pure silica sample is shown.

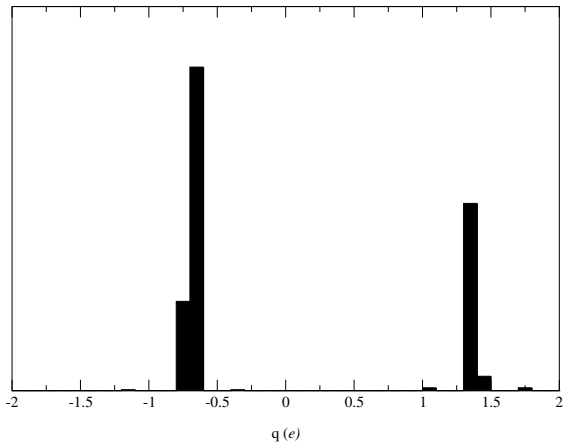

Figure 1. Charge histogram for a pure vitreous silica sample, consisting of 216 SiO2 units. The negative side of the graph corresponds to the charge distribution of oxygen. The positive side corresponds to that of silicon. Note the narrow charge distribution in both cases.

The narrow charge distribution at about –0.7*e* for oxygen and at about +1.4*e* for silicon reveals a quasi complete absence of defects in the network, such as dangling oxygens. On the other hand, when 20% Li_2O is added, charge distribution charges dramatically:

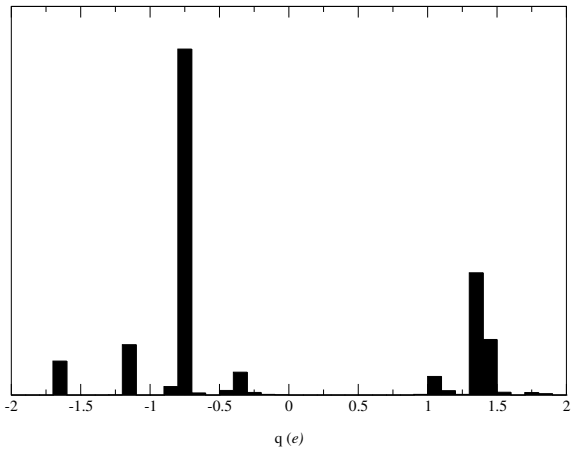

Figure 2. Charge distribution for a lithium tetrasilicate sample after MD run. Note the charge distribution broadening in both cases, and its concentration in discrete regions. Li^+ charges are not shown.

Charge distribution not only broadens, but also it concentrates in discrete regions. This fact implies the existence of different structural functionalities for the same chemical species. For the case of oxygen, the most numerous variety is the bridging one and exists in a charge subregion within $-0.5e$ and $-e$. Dangling oxygens have a charge within the $-e$ and $-1.5e$ interval. These charge regions were in part previously identified in Ref. 7. Other parts of the charge histogram were not studied therein owing to the fact that, at low concentrations, network disruption is not so evident from charge distribution. This is the case for both ends of the charge histogram.

The rightmost part of the oxygen charge histogram, where $q>-0.5e$, corresponds to *tricoordinated* oxygens, tantamount to "tricluster" oxygens[10,11], "triply-bonded" oxygens[3] and $^{[3]}O^{12}$. Tricoordinated oxygens are surrounded by 3 coplanar silicon atoms, and they seem to have remained elusive to experimental quantification in glassy silicates. In our tetrasilicate sample, tricoordinated oxygens amount to 6.6% of the total oxygen count. Other reported MD values are ~0.5% for mixed-alkali silicates[13] and 4-7% for $NaAlSi_3O^{12}$.

On the leftmost region of the oxygen charge histogram, where $q<-1.5e$, there exist *free* oxygens, which account for 7.2% of the total oxygen count. Free oxygens have no silicon neighbour, therefore they are no longer part of the tridimensional silica polymer, but rather they tend to situate themselves close to alkali cations (lithium, in the case of this study). In the MD literature of glassy silicates, a systematic treatment of free oxygen is not often encountered. In some reports, however, the presence of free oxygens is indirectly determined from stoichiometric relationships based on experimental measurements[14,15]. It is pertinent to note that the expected free oxygen concentration for lithium tetrasilicate should be around zero[16,17].

Silicon charge-structural function differentiation also occurs in a manner similar to the oxygen case, as Fig. 2 suggests. Whereas silicon is always part of the silica polymer, its oxygen coordination varies together with its charge. Therefore, it is to be expected that the different zones in the silicon charge histogram correspond to silicon atoms with 3, 4 or 5 neighbouring oxygens.

Conclusions

Charge-transfer MD simulations provide results that are arguably richer in details as their fixed-charge counterparts. It has been shown that, in a charge-transfer MD simulation it is possible to distinguish among different oxygen functionalities in a glassy silicate solely on the basis of charge. Whereas the results presented herein can be improved, the main purpose of this brief account is to offer a qualitative view of oxygen speciation in glassy lithium silicate.

[1] J. S. Jen and M. R. Kalinowsky, Journal of Non-Crystalline Solids **38&39**, p. 21 (1989).

[2] H. Melman and S. H. Garofalini, Journal of Non-Crystalline Solids **255**, p. 107 (1991).

[3] C. Huang and A. N. Cormack, Journal of Chemical Physics **93**, p. 8181 (1990).

[4] S. Balasubramanian and K. J. Rao, Journal of Physical Chemistry **98**, p. 10871 (1994).

[5] S. H. Garofalini and D. M. Zirl, Journal of Vacuum Science and Technology **A6**, p. 975 (1988).

[6] X. Yuan and A. N. Cormack, Journal of Non-Crystalline Solids **283**, p. 69 (2001).

[7] A. Alavi, L. J. Alvarez, S. R. Elliott and I. R. McDonald, Philosophical Magazine **B65**, p. 489 (1992).

[8] L. G. Cota, G. Vega, R. Correa and L. J. Alvarez, Molecular Simulation **20**, p. 315 (1998).

[9] B. Tischendorf, C. Ma, E. Hammerstein, P. Venhuizen, M. Peters, M. Affatigato and S. Feller, Journal of Non-Crystalline Solids **239**, p. 197 (1998).

[10] E. D. Lacy, Physics and Chemistry of Glasses **4**, p. 234 (1963).

[11] J. A. Tossell and R. E. Cohen, Journal of Non-Crystalline Solids **286**, p. 187 (2001).

[12] D. J. Stein and F. J. Spera, American Mineralogist **80**, p. 417 (1995).

[13] C. Huang and A. N. Cormack, Journal of Materials Chemistry **2**, p. 281 (1992).

[14] N. Iwamoto, N. Umesaki, M. Takahashi, M. Tatsumisago, T. Minami and Y. Matsui, Journal of Non-Cristalline Solids **95&96**, p. 233 (1987).

[15] J. Kieffer and C. A. Angell, Journal of Chemical Physics **90**, p. 4983 (1989).

[16] H. Maekawa , T. Maekawa, K. Kawamura and Toshio Yokokawa, Journal of Non-Crystalline Solids **127**, p. 53 (1991).

[17] N. Umesaki, M. Takahashi, M. Tatsumisago and T. Minami, Journal of Materials Science **28**, p. 3473 (1993).